Biomedical Signal Processing and Control 31 (2017) 272–287

Contents lists available at ScienceDirect

Biomedical Signal Processing and Control

journal homepage: www.elsevier.com/locate/bspc

Separating the effect of respiration on the heart rate variability using Granger's causality and linear filtering

Gustavo Lenis[a,*,1], Michael Kircher[a,1], Jesús Lázaro[b,c], Raquel Bailón[b,c], Eduardo Gil[b,c], Olaf Doessel[a]

[a] Institute of Biomedical Engineering (IBT), Karlsruhe Institute of Technology (KIT), Fritz-Haber-Weg 1, 76131 Karlsruhe, Germany
[b] Biomedical Research Networking Center in Bioengineering, Biomaterials and Nanomedicine (CIBER-BBN), Zaragoza, Spain
[c] Biomedical Signal Interpretation and Computational Simulation (BSICoS) Group, Aragón Institute of Engineering Research, IIS Aragón, University of Zaragoza, Zaragoza, Spain

ARTICLE INFO

Article history:
Received 6 March 2016
Received in revised form 12 July 2016
Accepted 28 July 2016

MSC:
00-01
99-00

Keywords:
ECG
Respiration
Heart rate variability
Coupling
Granger's causality
ARMAx filter

ABSTRACT

Heart rate variability (HRV) plays an important role in medicine and psychology because it is used to quantify imbalances of the autonomic nervous system (ANS). An important manifestations of the ANS on HRV is also directly related to respiration and it is called respiratory sinus arrhythmia (RSA). This is a controlled phenomenon that leads to a synchronized coupling between respiration and instantaneous heart rate. Thus, the portion of HRV that is not related to respiration, and could potentially contain undiscovered diagnostic value, is overlapped and remains hidden in a standard HRV analysis. In such cases, a decoupling procedure would deliver a discriminated HRV analysis and possible new insights about the regulation of the cardiovascular system. In this work, we propose an algorithm based on Granger's causality to measure coupling between respiration and HRV. In the case of significant coupling, we estimate and cancel the respiration driven HRV component using a linear filtering approach. We tested the method using synthetic signals and prove it to deliver a reliable coupling measurement in 96.3% of the cases and reconstruct respiration free signals with a median correlation coefficient of 0.992. Afterwards, we applied our method to signals recorded during paced respiration and during natural breathing. We demonstrated that coupling is dependent on respiratory frequency and that it maximizes at 0.3 Hz. Furthermore, the HRV parameters measured during paced respiration tend to level among subjects after decoupling. The intersubject variability of HRV parameter is also decreased after the separation process. During natural breathing, coupling is notoriously lower to non-existing and decoupling has little impact on HRV. We conclude that the method proposed here can be used to investigate the diagnostic value of respiration independent HRV parameters.

1. Introduction

The continuous change and adaptation of the instantaneous heart rate to internal and external factors is called heart rate variability (HRV). The regulation of the heart rate is carried out by the two complementary branches of the autonomous nervous system (ANS), the sympathetic and parasympathetic nervous system [1]. A healthy heart that is regulated in the proper manner is characterized by a strong HRV [2]. This principle is used in many fields of medicine and psychology for diagnostic purposes [3,4]. Scientific studies dealing with topics such as the quantification of risk of sudden cardiac death in patients with chronic heart failure or the assessment of mental workload when performing a given cognitive task, have been approached using the analysis of standard HRV parameters [5,6].

It is well known that HRV is strongly related to respiration [7,8]. There are two major reasons for this fact. First, respiration, heart rate and blood pressure are all part of a greater cardiorespiratory system that is also regulated by the ANS in the form of a coupled feedback control system [9]. Therefore, internal or external perturbations in one of the members of the system have a direct impact on the others. So for example, heart rate tends to increase as a response to hypoxia or hypercapnia in healthy subjects [10]. Another example is the baroreceptor reflex in which a change in blood pressure affects heart rate through negative feedback [11]. Second, a phenomenon called respiratory sinus arrhythmia (RSA),

* Corresponding author.
E-mail address: publications@ibt.kit.edu (G. Lenis).
URL: http://www.ibt.kit.edu (G. Lenis).
[1] These authors contributed equally to this work.

http://dx.doi.org/10.1016/j.bspc.2016.07.014
1746-8094/

in which heart rate increases during inspiration and it lowers during expiration, leads also to a notorious synchronized coupling between the breathing pattern and heart rhythm. As a matter of fact, RSA is the most important manifestation of the ANS directed to the heart and recorded non-invasively from the heart period [12]. Even though RSA is not fully understood, it is believed to minimize mechanical work done by the heart while maintaining a healthy concentration of gases in the blood and to optimize gas exchange while breathing by matching perfusion to heart rate [13–15]. Since the impact of RSA can change depending on different factors such as age, breathing frequency, tidal volume or general health condition of the subject [16–18], it is hard to quantify its effect on the HRV parameters. For this reason, other authors have tried to control the effect of respiration on HRV and have evaluated if this procedure can increase the diagnostic power of HRV parameters [19,20].

In a study presented in 2011 [21], the authors addressed the problem of detecting mental stress during a cognitive task using HRV. For this purpose, a transfer function, that described the cardiorespiratory coupling, was estimated and the respiration related fluctuations of the heart rate were subtracted. It was shown that separating the HRV analysis and removing the respiration driven part of it, leads to a residual HRV that is more suited for discrimination between mental stress and resting state. This conclusion has been ratified in other studies dealing also with stress classification and applying similar procedures [22,23].

The algorithms used to separate respiration from HRV presented in literature lack two important aspects. First, they do not quantify the strength of coupling between respiration and HRV. Thus, in the case that no significant coupling is present, a separation is still carried out. This has the risk of generating wrongly decoupled time series. In addition, the strength of the cardiorespiratory coupling could deliver more information about the state of health of the subject. Second, even though the methods presented in the past have been validated empirically, no validation on a theoretical basis has been carried out. Since the golden truth about the respiration related part of heart rate is not known, it is hard to evaluate the correctness and performance of the separating method itself.

In order to address these issues, we developed a method to quantify coupling between respiration and HRV using Granger's causality and defined a threshold to detect significant coupling. The algorithm then continues with the separation of the respiration induced part of the HRV. Special procedures were created for paced respiration at different frequencies and natural breathing. The residual HRV unrelated to respiration is achieved using linear filters such as an optimal notch filter (for paced respiration) and an ARMAx filter (for natural breathing). Similar methodologies used for related applications have been presented in the past in [24,21]. For the purpose of testing the method on a theoretical basis, we also carried out a simulation study using synthetic signals that resembled the ones measured for this work. Finally, after demonstrating the validity of the developed algorithm, we use it to separate the influence of respiration on the HRV in a data set recorded during paced respiration and in another one with natural breathing.

2. Methods

2.1. Data

2.1.1. Synthetic signals

In order to test the algorithms developed in this work at a theoretical level, we carried out a simulation study using synthetic signals. Respiration, RR time series (which is reciprocal of the instantaneous heart rate) and their coupling were modeled to resemble the real measured signals in the time and frequency domain. The block diagram shown in Fig. 2a displays the complete simulation scheme that includes the generation of realistic time series, the way these signals are coupled, the decoupling algorithm and the evaluation of the reconstruction. In this work, we call *intrinsic* the part of HRV that is not related to respiration, because it cannot be recorded independently and might be overlapped by other larger influences such as RSA. The intrinsic RR time series $RR_{intri}(n)$ is modeled using pink Gaussian noise [25]. This series resembles the theoretical RR time series that is free of any influence from respiration. The respiration signal $resp(n)$ is modeled using a harmonic function with time varying frequency. In order to model coupling, the respiration signal is first filtered by a moving average (MA) system $G(k)$ and added to the intrinsic RR time series [21]. The resulting signal represents the measured RR time series $RR_{meas}(n)$ that would have been computed from the recorded ECG. This model is characterized by an open-loop configuration allowing an external input. This is a specific case of the more general family of multivariate dynamic adjustment (MDA) models [26].

Mathematically speaking, the signals are modeled in the following way:

- The intrinsic RR time series is modeled by random Gaussian pink noise. It is characterized by a spectral power density that is proportional to the reciprocal of the frequency $S_{RR_{intri}}(f) \propto 1/f$ and by a normal amplitude distribution $\mathcal{N}(0;\sigma)$ in the time domain. This signal can be achieved by filtering white Gaussian noise with a low pass filter [27].
- Respiration is modeled with a harmonic function of the general form $resp(n) = A \cdot cos(\varphi(n))$. The time varying phase of the cosine function is defined as a time discrete approximation of the integral of the time varying frequency $f(n)$:

$$\varphi(n) = 2\pi \sum_{k=0}^{n} \frac{f(k)}{f_s}$$

where f_s is the sampling frequency in Hz used in the real signal processing algorithm. In our study, f_s was set to be 4 Hz, which is a typical value used in literature [28]. The time varying frequency $f(n)$ is defined using the hyperbolic tangent (tanh) function which has a sigmoid shape. The function is parametrised to have lower and upper bounds $f_0 - f_1$ and $f_0 + f_1$ and time discrete constant $f_s \cdot T$. It is centered at the sample point n_0:

$$f(n) = f_0 + f_1 \cdot \tanh\left(\frac{n - n_0}{f_s \cdot T}\right)$$

The parameters A, f_0, f_1, T and n_0 can be freely chosen by the user to recreate different scenarios. In this work, we investigated two types of respiration signals, the constant and the natural breathing. In the case of constant breathing, the frequency f_0 comes randomly from the interval $f_0 \in [0.1;0.6]$ Hz and $f_1 = 0.005$ Hz is chosen fixed to ensure that spectral power is localized around f_0. In the case of natural breathing, the frequency f_0 is also randomly chosen from the interval $f_0 \in [0.1;0.6]$ Hz and f_1 is an aleatory variable from the interval $f_1 \in [0;0.1]$. For both types of signals, the other parameters present in the sigmoid function were randomly chosen from the following intervals: $A \in [0.2;5]$, $n_0 = [180;540]$, $T \in [10;30]$ s and a signal length of $N = 720$ sample points, or three minutes, was set fixed. A large number of repetitions was performed and statistics were carried out for evaluation purposes. The simulation study is presented in detail in Section 3.

The chosen parameters are in accordance with the signals included in the two studies presented in this work, which facilitates the comparability between results obtained from simulation and real measurements. Furthermore, the parameters are

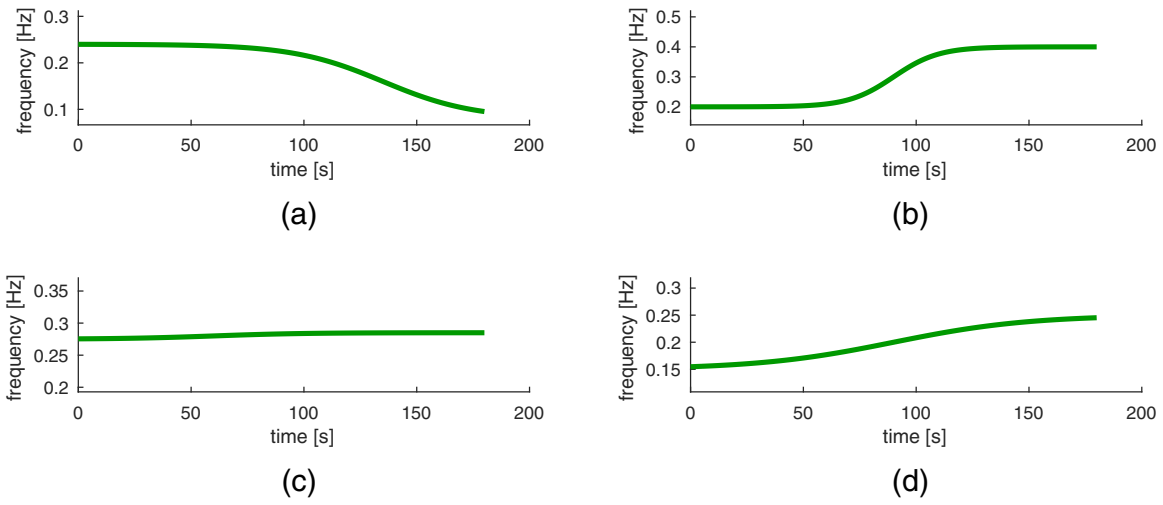

Fig. 1. Four different realizations of time dependent breathing frequencies with different combinations of the simulation parameters. The following parameters were used: (a) $f_0 = 0.16$ Hz, $f_1 = 0.08$ Hz, $n_0 = 540$, $T = 20$ s. (b) $f_0 = 0.3$ Hz, $f_1 = 0.1$ Hz, $n_0 = 360$, $T = 10$ s. (c) $f_0 = 0.28$ Hz, $f_1 = 0.005$, $n_0 = 480$, $T = 20$ s. (d) $f_0 = 0.2$ Hz, $f_1 = 0.05$ Hz, $n_0 = 360$, $T = 30$ s.

also in accordance with typical values reported in literature [29] which gives the method a general applicability. Fig. 1 shows four examples on how different combinations of the parameters can produce a large variety of time depending breathing frequencies that account for many real life scenarios.

- The coupling filter $G(k)$ bring the intrinsic RR time series, the respiration and the measured RR time series together. The following mathematical model is used to represent this behavior:

$$RR_{meas}(n) = \sum_{k=1}^{K} g(k) \cdot resp(n-k) + RR_{intri}(n)$$

where K is the order of the filter and $g(k)$ are the filter coefficients. In our simulation study, the system order was always chosen $K \leq 12$. By doing so, we allowed coupling behavior from respiration values up to three seconds in the past [30].

Fig. 2b to 2i shows an example of the kind of signals generated using the simulation protocol and the reconstruction algorithm proposed here. A representation in the time domain together with the power spectral density (PSD) are given. Note how the coupled RR time series (time and frequency domain) has a shape that arises from both, the intrinsic RR time series and the respiration signal. Finally, the decoupled RR time series is again very similar to the original intrinsic RR time series. This example shows how the decoupling algorithm performed in the desired manner.

Furthermore, a comparison with real measurements from the other data sets used in this work can be seen in Fig. 3.

2.1.2. Paced respiration study

The paced respiration study (PRS) was conducted by the group BSICoS at the university of Zaragoza in Spain. 19 subjects (13 male and 6 female), including undergraduate and graduate students, PhD candidates and researches from the group were enrolled. Subject ages ranged from 21 to 52 years (median of 28 years). The subjects were asked to breath at a constant respiration rate for 3 min and to take a short break afterwards. The breathing frequency was held constant during every breathing session but increased from one session to the next one. Breathing rate ranged from 0.1, 0.2, ..., to 0.6 Hz. In order to ensure the breathing rate was truly constant, a video displaying an oscillating sine wave at the given frequency was presented to the subject, so that they were able to follow the pattern with their breathing. Subjects breathed at the frequency of the sine wave in the video with a small error of 0.22 ± 1.05 mHz [31].

ECG and respiratory data were recorded simultaneously using the devices ABP-10 and POLY-37 from the manufacturer Medicom MTD. Both signals were recorded at a sampling rate of 1000 Hz and were digitized with a resolution of 24 bits. ECG was recorded using three channels and orthogonal electrode placement. Respiration effort was acquired using a chest belt and at a sampling rate of 250 Hz. Signal quality was visually inspected prior to any processing algorithm. One subject had to be removed from the study because large portions of the data were missing or had very low signal quality.

In order to avoid errors related to aliasing throughout the analysis carried out with this data set, the subjects not fulfilling the Shanon sampling theorem were also removed from the study. First, a subject was considered to "violate" the sampling theorem if their mean heart rate was smaller than twice their breathing frequency. Subjects potentially leading to aliasing errors appeared only for the breathing frequencies 0.5 and 0.6 Hz. In the case of 0.5 Hz, three subjects had to be removed from the analysis while for 0.6 Hz there were nine subjects not fulfilling the sampling theorem.

Fig. 3 shows an example of the signals recorded in the PRS study. In the same figure, as comparison, an example of synthetic signals generated to reproduce the recorded signals in a realistic manner is displayed. The power spectrum of both, the synthetic and simulated signals, can also be seen in Fig. 3.

The data recorded in the PRS study were used previously for a different research project presented at the conference Computing in Cardiology 2014 in Cambridge, Massachusetts [31].

2.2.. Fantasia database

The PRS study has the drawback of not having any records of subjects breathing naturally. In order to fill this gap, we used the data from the Fantasia database which is part of the repository of physionet.org [32,33]. The data were acquired from 20 young and 20 old subjects. For the young subjects, ages ranged from 21 to 34 years. Old subjects were between 68 and 85 years old. Each subgroup consisted of an equal amount of female and male subjects. One ECG channel together with a respiration effort signal is present in this data set. Both signals were acquired at a sampling rate of 250 Hz for an interval of 120 min while the subjects were watching the Disney movie Fantasia in a resting supine position. The breathing pattern of the subjects is considered to be natural.

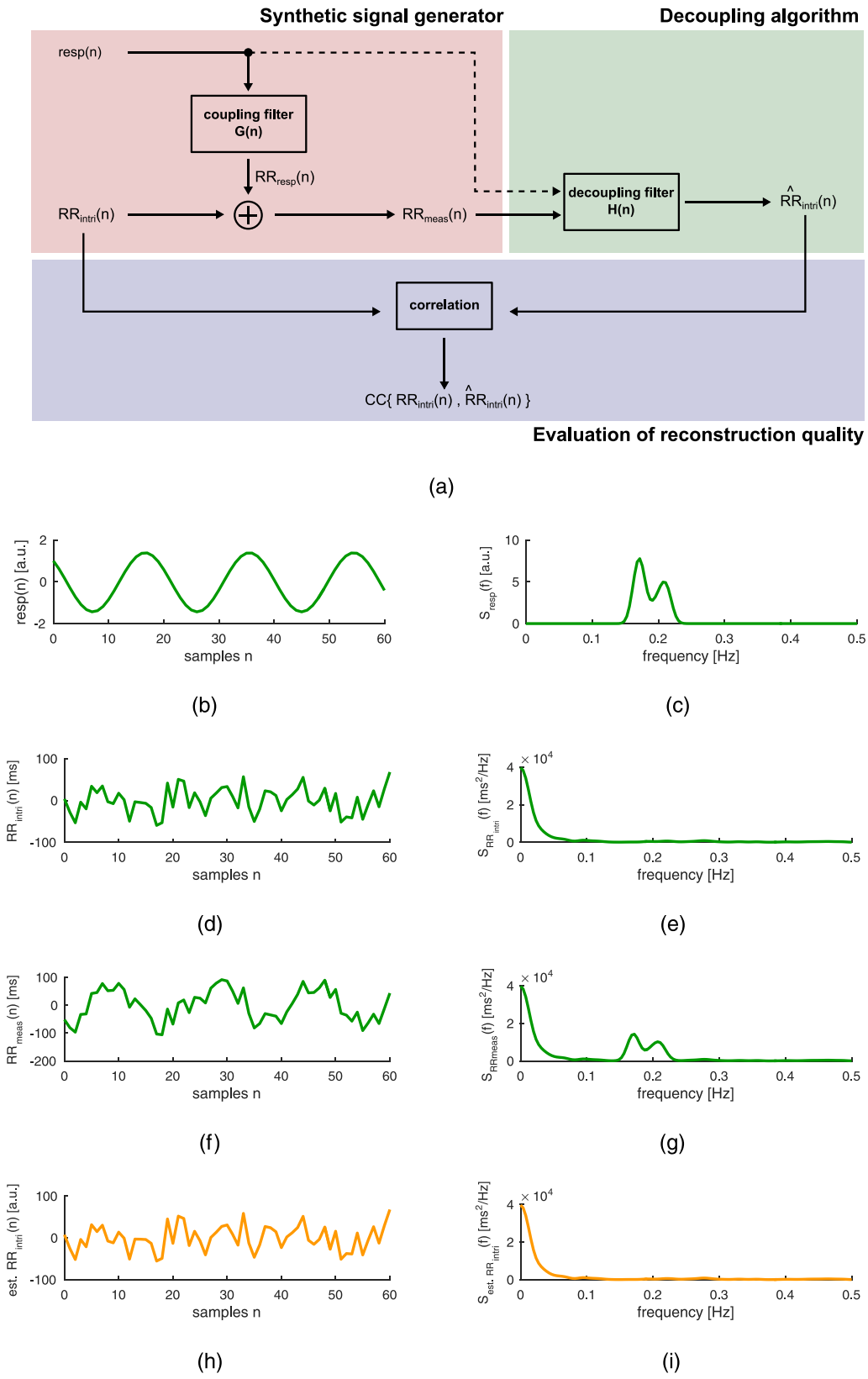

Fig. 2. (a) Simulation scheme used to create synthetic signals for theoretical testing of the algorithms used in this work. (b) A portion of a synthetic respiration signal. (c) PSD of the complete respiration signal used for (b). (d) A portion of a synthetic intrinsic RR time series. (e) PSD corresponding to the complete RR time series used for (d). (f) A portion of an RR time series after respiration has been coupled. (g) PSD of the complete RR time series used for (f). (h) A portion of the decoupled RR time series using one of the algorithms developed in this work. (i) PSD of the decoupled RR time series.

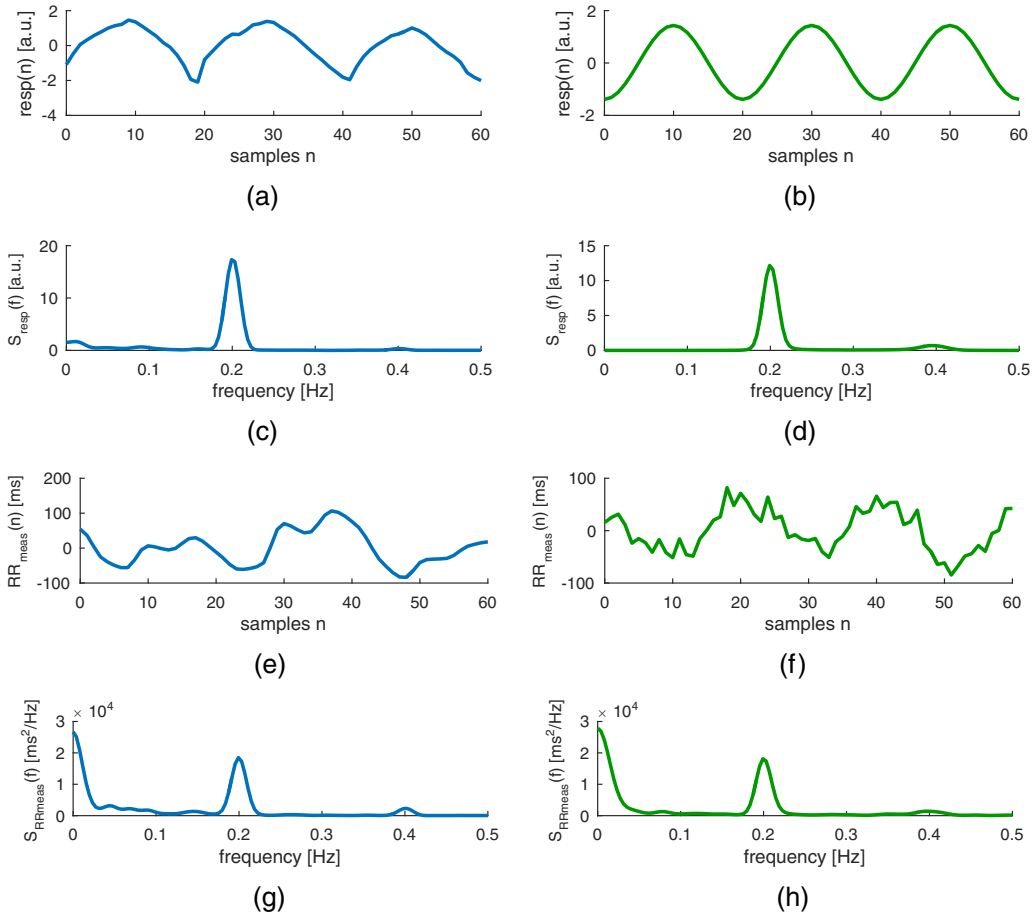

Fig. 3. Comparison between signals recorded in the PRS study (left column) and synthetic signal used in the simulation study (right column). (a) A portion of the filtered respiration signal as it was recorded from a subject in the PRS study. (b) A portion of a synthetic respiration signal generated to have similar properties as the one used for (a). (c) PSD of the complete respiration signal used for (a). (d) PSD of the complete respiration signal used for (b). (e) A portion of the recorded RR time series from the same subject in the PRS study. (f) A portion of the synthetic RR time series generated to have similar properties as the signal used for (e). (g) PSD of complete RR time series signal used for (e). (h) PSD of the complete RR time series signal shown in (f).

Fig. 4 shows an example of the signals recorded in the Fantasia database. In the same figure, as comparison, an example of synthetic signals generated to recreate the measurements in a realistic manner. The power spectrum of both, the recorded and synthetic signals, can also be seen in Fig. 4.

2.3. Filtering the ECG and respiration signals

ECG signals are typically corrupted by low frequency baseline wander, high frequency random noise or muscle movement and power line interference. Baseline wander was filtered using a high pass Butterworth filter with a cutoff frequency of 0.5 Hz. In order to reduce high frequency random noise, every signal was filtered with a low pass Butterworth filter with a cutoff frequency of 250 Hz [34,35]. Power line interference was removed using a Gaussian notch filter located at 50 Hz or 60 Hz and all its harmonics [36].

Regarding the respiration signal, baseline wander was removed with a high pass Gaussian filter with a cutoff frequency of 0.05 Hz. High frequency random noise is attenuated using a low pass Butterworth filter with a cutoff frequency of 20 Hz. Power line interference was removed using again a Gaussian notch filter located at 50 Hz or 60 Hz and all its harmonics.

2.4. Processing the ECG signal

The signal processing work flow starts with the ECGs previously filtered and the detection of the QRS complexes. The algorithm used for this purpose is based on the stationary wavelet transform (SWT). The detail coefficients at level 2 are computed and compared against an adaptive threshold. Signal portions above the threshold are detected as QRS complexes. The most significant peak inside the QRS complex is then labeled as the R peak [37]. The time distance between two subsequent R peaks is referred as RR interval. A collection of successive RR intervals is called RR time series. In this study, we removed the mean of every RR time series so that it oscillates around zero.

In the case that more than one ECG channel per subject is present in the data set, a synchronization of information among channels is carried out. This way, wrong detections or false annotations caused by local artifacts or strong noise can be reduced. Using this procedure, we ensure that if a wrong detection takes place in one of the channels, it can be corrected using the other two.

Artifacts in the RR time series can always be present. They lead to an erroneous point in the series and must be removed. For this purpose we use the method presented by Malik [38] that removes an RR interval if it differs in more than 20% from the previous or subsequent one.

2.5. Coupling measures between respiration and RR time series

In this work, we propose the quantification of coupling between the measured RR time series and the respiration signal using the Granger's causality. It is described as follows.

2.5.1. Granger's causality

The way Granger approaches causality can be summarized in the following manner: A time series $y(n)$ is considered to cause another series $x(n)$, if the prediction of the second series can be improved by introducing information from the first one. The prediction of the series $x(n)$ is performed using a linear autoregressive (AR) model. The introduction of the information coming from the exogenous time series $y(n)$ is carried out using a linear moving average model (MAx) and tested to deliver a statistically significant improvement in the estimation. The improvement is quantified by comparing the variance of the estimation including and not considering the exogenous input [39]. Mathematically speaking, the Grager's causality can be formulated as follows:

The time series $x(n)$ is first modeled as an AR stochastic process.

$$x(n) = \sum_{k=1}^{P} a(k) \cdot x(n-k) + \epsilon_{AR}(n)$$

The prediction error $\epsilon_{AR}(n)$ is assumed to be normally distributed with expected value μ_{AR} and variance σ^2_{AR}. The expected value of the prediction error is typically zero, so that its variance is given by:

$$\sigma^2_{AR} = \frac{1}{N-P-1} \sum_{k=1}^{N} \epsilon^2_{AR}(n)$$

where N is the total amount of points recorded from the time series. The estimated variance σ^2_{AR} is also a random variable governed by a χ^2_{N-P} distribution. After the AR estimation, the information from the exogenous input is then added to the prediction:

$$x(n) = \sum_{k=1}^{P} a(k) \cdot x(n-k) + \sum_{k=1}^{Q} b(k) \cdot y(n-k) + \epsilon_{ARMAx}(n)$$

The variance σ^2_{ARMAx} is χ^2_{N-P-Q} distributed. The two residual variances are then compared building their normalized difference [40]:

$$\gamma_{yx} = \frac{\sigma^2_{AR} - \sigma^2_{ARMAx}}{\sigma^2_{ARMAx}} = \frac{\sigma^2_{AR}}{\sigma^2_{ARMAx}} - 1$$

The ratio $\sigma^2_{AR}/\sigma^2_{ARMAx}$ is a random variable that follows the F-distribution with $N-P$ and $N-P-Q$ degrees of freedom. The null hypothesis that $y(n)$ does not cause $x(n)$ can be statistically tested by applying an F-test and allowing an error probability of maximal 5%. The threshold for the statistical significance demonstrating an increase in the prediction can be computed by

$$\gamma^{5\%}_{yx} = F^{-1}(0.05, N-P, N-P-Q) - 1$$

where F^{-1} denotes the inverse of the F-distribution. In particular, the value $\gamma_{yx} = 0$ means that absolutely no coupling was found. Higher values indicate increasing coupling and if the given

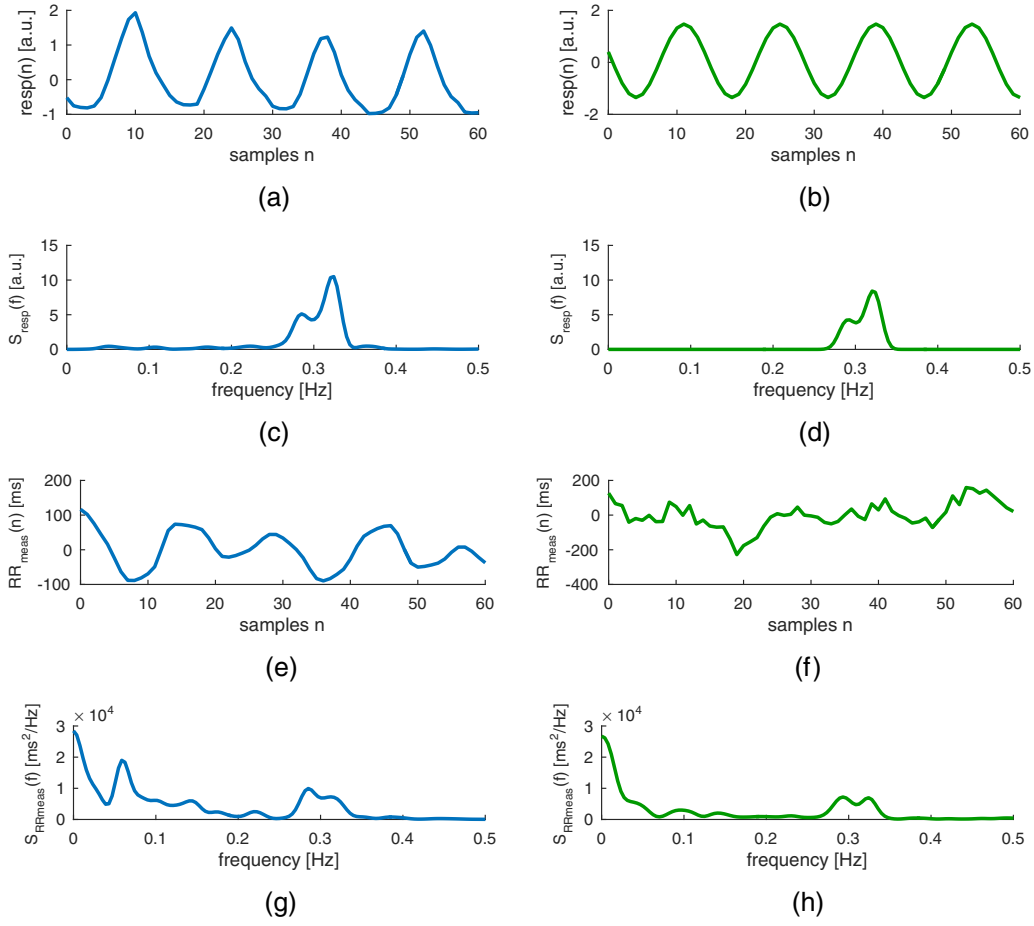

Fig. 4. Comparison between signals recorded in the Fantasia database (left column) and synthetic signal used in the simulation study (right column). (a) A portion of the filtered respiration signal as it was recorded from a subject in the Fantasia database. (b) A portion of the synthetic respiration signal generated to have similar properties as the one used for (a). (c) PSD of the complete respiration signal used for (a). (d) PSD of the complete respiration signal used for (b). (e) A portion of the recorded RR time series from the same subject in the Fantasia database. (f) A portion of the synthetic RR time series generated to have similar properties as the one used for (e). (g) PSD of complete RR time series signal used for (e). (h) PSD of the complete RR time series signal used for (f).

threshold $\gamma_{yx}^{5\%}$ is surpassed, the coupling is said to be statistically significant.

Another important aspect are the parameter P and Q used in the linear regressions must be given also. In this work, we use the Bayesian Information Criterion (BIC) to find an optimal estimation for the model orders P and Q [41]. In this method, the following cost function is minimized to find the AR model order P:

$$BIC_{AR}(P) = N \cdot \ln(\sigma_{AR}^2) + P \cdot \ln(N)$$

The model order Q for the MA part of the prediction is found analogously. In the case that no minimum is found, the optimization process is slightly modified to find a "best guess" and carried out in the same manner described in [42]. Finally, in our application, $x(n)$ is replaced by the measured RR time series $RR_{meas}(n)$ and $y(n)$ represents the respiration time series $resp(n)$. It is also important to mention that the separation of the intrinsic and respiration driven RR time series is only carried out, if significant coupling has been detected. Otherwise, it is assumed that no significant coupling is present and thus no separation is needed.

2.6. Separation in the case of paced respiration

The idea behind the separation in the case of paced respiration relies on the fact that the power spectrum of HRV is characterized by one strong peak located at the constant breathing frequency. Therefore, it should be possible to remove that peak applying a notch filter [43]. In this work, we present a new method that consists in approximating the peak at the breathing frequency using a Gaussian bell and inverting that bell to create a notch filter that removes the peak without compromising the rest of the spectrum. The approximation of the peak is performed using a least squares estimation and the spectrum is obtained using the Welch's method [44]. It was performed using a Hamming window of 64 s (256 sample points). An overlap of 128 samples between neighboring windows was chosen and zero padding was used to extend the number of samples for the Fourier transform to $2^{10} = 1024$ sample points.

The estimation problem can be formulated as follows:

$$\left|S_{RR}(k) - S_{Gauss}(k)\right|^2 \rightarrow \min \qquad \text{for} \quad k \cdot \Delta f \in B_{\min}$$

$$\left|S_{RR}(k) - \mathbf{a} \cdot \exp(-\mathbf{b} \cdot (k \cdot \Delta f - f_{resp})^2)\right|^2 \rightarrow \min \quad \text{for} \quad k \cdot \Delta f \in B_{\min}$$

In these equations, $S_{Gauss}(k)$ is the Gaussian bell function in spectrum with parameters $\mathbf{a}$ and $\mathbf{b}$ that are going to be estimated. f_{resp} is the constant breathing frequency that corresponds to the maximum of the local spectral peak. k is the positive integer variable in the Fourier domain and B_{min} is the band spanned from the first local minimum prior to the peak to next local minimum after the peak. It can be observed from the formulation of the problem that the parameters do not have a linear dependency of the optimization function. Therefore, the logarithm is applied to each of the spectra that creates a linear signal model. In that case we have:

$$\left|\ln(S_{RR}(k)) - \ln(\mathbf{a} \cdot \exp(-\mathbf{b} \cdot (k \cdot \Delta f - f_{resp})^2))\right|^2 \rightarrow \min \quad \text{for} \quad k \cdot \Delta f \in B_{\min}$$

$$\left|\ln(S_{RR}(k)) - \ln(\mathbf{a}) + \mathbf{b} \cdot (k \cdot \Delta f - f_{resp})^2\right|^2 \rightarrow \min \qquad \text{for} \quad k \cdot \Delta f \in B_{\min}$$

The parameters $ln(\mathbf{a})$ and $\mathbf{b}$ can be obtained from this formulation using the least squares approach. By inverting the obtained Gaussian bell, the decoupling notch filter $H(k)$ is achieved:

$$|H(k)|^2 = \mathbf{a} \cdot (1 - \exp(-\mathbf{b} \cdot (k \cdot \Delta f - f_{resp})^2))$$

The filtering process is performed in the time domain to reduce artifacts at the boundaries of the signal that can arise because of circular convolution. Fig. 5 shows the estimation process in the frequency domain together with the notch filter and the coupled and respiration free signal obtained from the RR time series. This method has the advantage of being applicable even if no respiration signal was recorded. However, it can only work if the respiration frequency is known and can be assumed to be constant so that one peak centered at the respiratory frequency arises in the power spectrum of the RR time series. However, even then, it is possible that the Gaussian notch filter removes too little or too much from the spectrum of the RR time series.

2.7. Separation in the general case

In the general case of spontaneous breathing, it cannot be assumed that the respiration rate is constant. Therefore, a new approach must be taken to decouple respiration from RR time series. The idea proposed in this paper is based on a decoupling MAx filter $H(k)$ and an accurate estimation of the respiration driven part of the RR time series. For this purpose, a linear transfer model with order Q is used. The filter coefficients are estimated using linear regression and the filter order is chosen using the BIC. The mathematical model is given by the following equation:

$$RR_{meas}(n) = \sum_{k=1}^{Q} h(k) \cdot resp(n-k) + RR_{intri}(n)$$

The estimation problem can then be formulated as follows:

$$\left|RR_{meas}(n) - \sum_{k=1}^{Q} h(k) \cdot resp(n-k)\right|^2 \rightarrow \min \quad \text{for} \quad h(k) \in \text{Re}$$

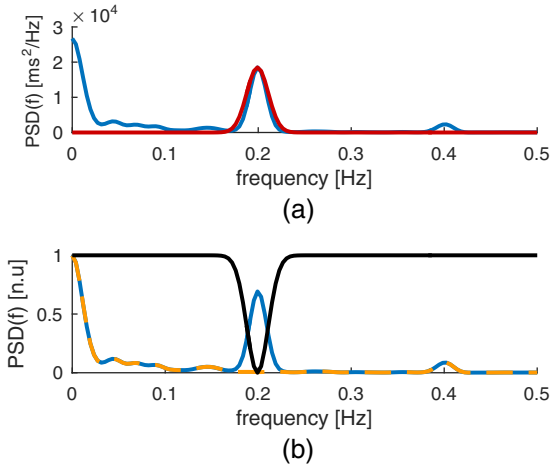

Fig. 5. Separation of respiration from RR time series using an estimated Gaussian notch filter. (a) Original PSD of the RR time series and estimated power coming from the respiration. A Gaussian bell is used for this purpose. (b) The estimated Gaussian bell is inverted and used as notch filter (black curve). The effect of respiration is suppressed after the filtering process (orange curve). (For interpretation of reference to color in this figure legend, the reader is referred to the web version of this article.)

The coefficients $h(k)$ can then be found using least squares minimization. The intrinsic RR time series can thus be reconstructed as:

$$\hat{RR}_{intri}(n) = RR_{meas}(n) - \sum_{k=1}^{Q} h(k) \cdot resp(n-k)$$

Fig. 6 shows an example of the time and frequency domain representations of a synthetic and a recorded RR time series for which the decoupling algorithm presented in this section was applied. The signals before and after the separation algorithm is applied, are displayed in this figure.

2.8. Simulation study to test the algorithm

In order to test the methods developed in this work on a theoretical basis, we designed two experiments using the synthetic signals introduced in Section 2.2. In the first experiment, we approached the question of detecting a significant coupling between respiration and RR time series. With the second experiment we evaluated the performance of the separation algorithms.

2.8.1. Evaluation of Granger's causality as a coupling measure

In order to test the coupling measure introduced here, we created a total of 200 000 realizations, each with a duration of 3 min ($N = 720$ samples). The parameter A, introduced in Section 2.2, is responsible for the amplitude of the simulated respiration signal and it is thus related to coupling strength. In order to measure the dependency of the parameter γ_{yx} from the coupling strength, we varied A in the following interval $A = \{0, 0.6, 1.4, 2.8, 5\}$. For $A = 0$ coupling is canceled out while for $A > 0$ coupling is present and becomes the strongest for $A = 5$. These values were chosen with the aim of recreating normal values of the LF/HF ratio that is known to be in the interval LF/HF $\in$ [0.2;5] [45].

For the case of no coupling ($A = 0$), 100 000 realizations were performed. The same amount of realization were created to investigate coupling ($A > 0$). In each one, the RR time series, the respiration signal (natural breathing) and the coupling filter $G(k)$ were varied randomly. The coupling filter was chosen to have a random order of maximal 12 and its coefficients were aleatory generated from the interval $[-1, 1]$.

2.8.2. Evaluation of the separation algorithms

In order to test the decoupling algorithms, we created a total of 100 000 realizations, each with a duration of 3 min ($N = 720$ samples). Half of the realizations were chosen to recreate paced respiration with an almost constant breathing frequency. The other 50 000 realization were generated to simulate natural breathing. Both signal types were created having randomly generated parameters exactly as described in Section 2.2. Decoupling was performed with the Gaussian notch filter and the MAx filter.

The aim of the developed algorithms is to reconstruct the original intrinsic RR time series $RR_{intri}(n)$ using the measured RR time series and the respiration signal. In order to quantify the quality of the reconstruction, we computed the correlation coefficient between the original intrinsic RR time series and the reconstructed intrinsic RR time $\hat{RR}_{intri}(n)$ series.

Mathematically speaking, the correlation coefficient is given by:

$$CC\{RR_{intri}(n), \hat{RR}_{intri}(n)\} = \frac{E\left\{\left(RR_{intri}(n) - E\left\{RR_{intri}(n)\right\}\right) \cdot \left(\hat{RR}_{intri}(n) - E\{\hat{RR}_{intri}(n)\}\right)\right\}}{\sqrt{E\left\{\left(RR_{intri}(n) - E\left\{RR_{intri}(n)\right\}\right)^2\right\} \cdot E\left\{\left(\hat{RR}_{intri}(n) - E\{\hat{RR}_{intri}(n)\}\right)^2\right\}}}$$

where $E\{\cdot\}$ denotes the expected value operator. The correlation coefficient is always a number between −1 and +1. Thus, it is an intuitive measurement of similarity. In the case of a perfect match, the number +1 is delivered. In the case of orthogonality, the correlation coefficient is zero.

2.9. Analysis of heart rate variability

An important goal of this research project was to compare HRV parameters before and after decoupling of respiration has been performed. Therefore, an HRV analysis is necessary. The processing of the measured RR time series begins with an interpolation of the series to a sample frequency of 4 Hz. The interpolation method used is the monotone cubic interpolation [46]. The interpolation process is necessary for three reasons. First, in order to perform HRV analysis in the frequency domain using the Welch's method, it is necessary to have equidistant points in the interpolated RR time series. In addition, increasing the resolution and total amount of points in the time domain series leads to a smoother estimation of the spectrum in the frequency domain. Second, in order to quantify coupling between RR time series and respiration, the same sampling frequency is needed in both signals. For this purpose, the respiration signal is downsampled to the same sampling rate of 4 Hz. An antialiasing filter with a cutoff frequency at 2 Hz is applied to the respiration signal prior to the downsampling process. Third, by choosing a monotone cubic interpolation, we ensure that no overshooting is present in the interpolated RR time series. Interpolation with overshooting creates higher RR intervals and could lead to false HRV parameters after the separation of the respiration driven oscillation has been carried out.

In order to quantify HRV, many parameters have been proposed in the literature [38,47]. In this work, we restrict the HRV analysis to seven well studied parameters, four from the time domain and other three from the frequency domain analysis. From the time domain, the parameters SDNN, rMSSD, TINN and Approximate Entropy (ApEn, $r = 0.2 \cdot SDNN$, $m = 2$ and $N = 720$) were calculated. All the time domain parameters obtained from the decoupled RR time series, were calculated by sampling the decoupled series to the original time points prior to the interpolation process. Thus, a valid comparison of HRV parameters before and after decoupling can be assumed.

In order to calculate the parameters from the frequency domain, a proper estimation of the power spectral density of the RR time series is needed. For this purpose, we used the Welch's method and a Hamming window of 64 s (256 sample points). An overlap of 50% between neighboring windows was chosen and zero padding was used to extend the number of samples for the transform to $2^{10} = 1024$ sample points. A spectral resolution of $\delta f = 3.91 \cdot 10^{-3}$ Hz is achieved. The transform was calculated using the Fast Fourier Transform (FFT) algorithm. From the frequency domain analysis, the parameters LF, HF and LF/HF ratio were computed.

The authors assume that using the group of HRV parameters presented in this section, an adequate quantification of the autonomous regulation of the heart can be achieved.

3. Results

3.1. Evaluation of Granger's causality as a coupling measure

Fig. 7a shows the boxplot displaying the value of the Granger's causality based measure γ_{yx} used to investigate coupling between the synthetic respiration signal and its corresponding RR time series in dependency of the coupling strength parameter A. The theoretical threshold $\gamma_{yx}^{5\%}$ for significant coupling is also displayed in the figure. This threshold was used to classify the 200 000 realizations

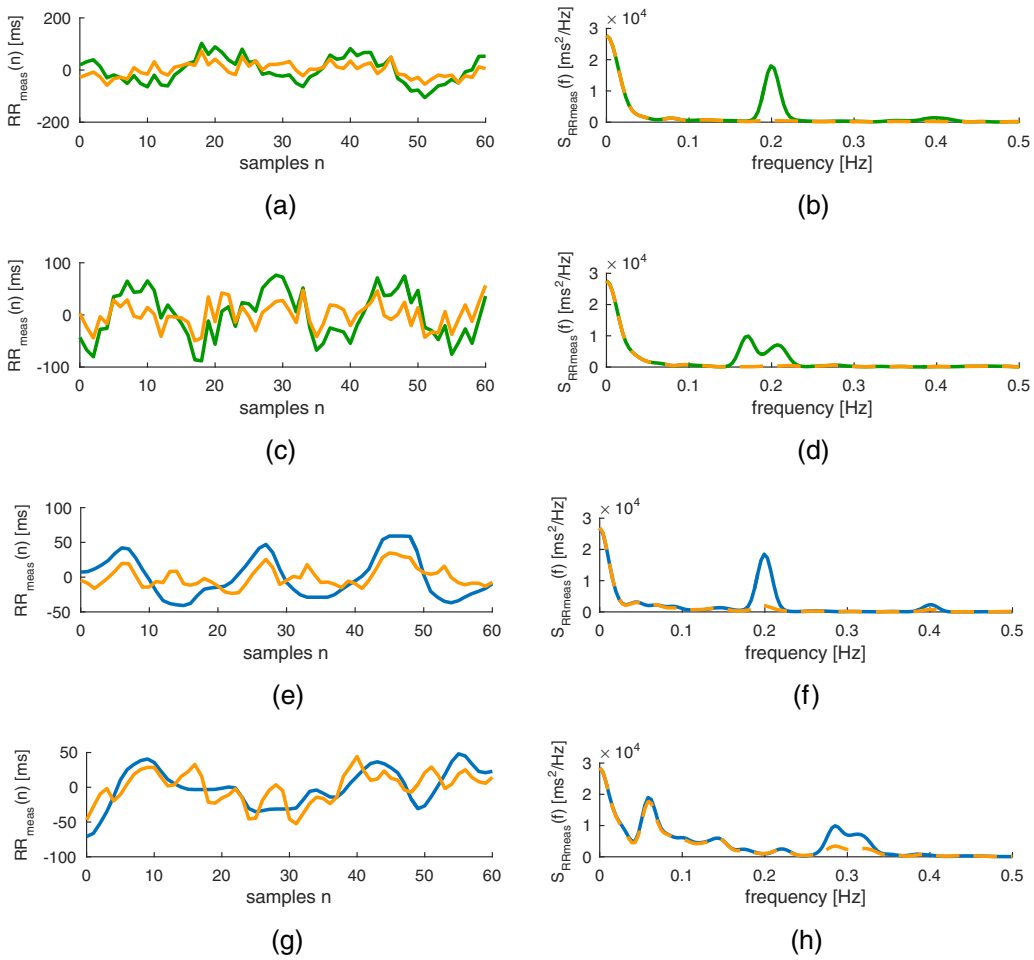

Fig. 6. (a) A portion of a synthetic RR time series with coupling constant breathing before (green) and after (orange) the MAx separation algorithm is applied. (b) PSD of the complete signals used for (a). (c) A portion of a synthetic RR time series with coupling natural breathing before (green) and after (orange) the MAx separation algorithm is applied. (d) PSD of the complete signals used for (c). (e) A portion of a real measurement of an RR time series with coupling constant breathing before (blue) and after (orange) the MAx separation algorithm is applied. f: PSD of the complete signals used for (e). (g) A portion of a real measurement of an RR time series with coupling natural breathing before (blue) and after (orange) the MAx separation algorithm is applied. (h) PSD of the complete signals used for (g). (For interpretation of reference to color in this figure legend, the reader is referred to the web version of this article.)

from the simulation study. According to the known golden truth, the classification system delivered a global correct rate of 96.3%, a sensitivity of 92.6%, a specificity of 100%, a positive predictive value of 100% and a negative predictive value of 93.1%. The majority of the classification errors were present in the lowest coupling ($A = 0.6$) for which the classification was wrong in 25.4% of the cases. An increasing of the median γ_{yx} was also observed with increasing parameter A.

3.2. Evaluation of the separation algorithms

Fig. 7b shows boxplots displaying the quality of the reconstructed intrinsic RR time series $\hat{RR}_{intri}(n)$ when compared to the original intrinsic RR time series $RR_{intri}(n)$ using the correlation coefficient. In the case of paced respiration, the reconstruction delivered by the Gaussian notch filter has a median of 0.968 which is slightly below the one obtained using the MAx filter. The 25th percentile of the boxplots are around 0.958 and 0.990, which demonstrates a reconstruction of high quality for both methods in at least 75% of the cases.

In the case of natural breathing MAx is notoriously better than the Gaussian notch. The MAx filter achieved a median of 0.992 and an interquartile range (IQR) of 0.008, which demonstrates a robust reconstruction of high quality for this method. The Gaussian notch filter achieved a median of 0.864 and an IQR of 0.111. Even though this filter was not developed for spontaneous breathing, its upper 75th percentile achieved a correlation coefficient of 0.931, which demonstrates that it can still be applicable in some cases of spontaneous breathing, for which the respiration rate remains relatively constant.

The results observed from the simulation study brought us to the conclusion that the MAx filter is the best choice for both applications. Therefore, we decided to use this method for the decoupling procedure carried out on the two databases analyzed in this work.

3.3. Coupling between RR time series and respiration

3.3.1. Paced respiration study

The results obtained for the Granger's causality based coupling measure γ_{yx} among all subjects in the PRS study are depicted as boxplots in dependency of breathing rate in Fig. 8. The threshold for significant coupling is also depicted in magenta. It can be observed that the median coupling among all subjects in the study is above threshold for all breathing frequencies except 0.6 Hz. The coupling strength grows with increasing frequency and reaches its highest value at 0.3 Hz. It then lowers and reaches its minimum at 0.6 Hz. At 0.3 Hz almost all subjects have a significant coupling between respiration and RR time series.

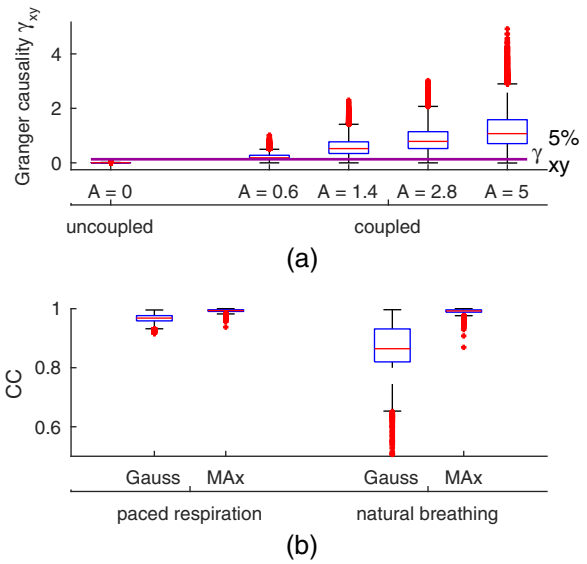

Fig. 7. Results of the simulation study. (a) The Granger's causality measure γ_{yx} was used to quantify strength of coupling between RR time series and respiration signals. For $A = 0$ no coupling is canceled out while for $A > 0$ coupling is present and becomes the strongest for $A = 5$. Coupling is classified as significant if γ_{yx} is above the given threshold. Coupling is correctly identified in 96.3% of the cases and achieves a sensitivity of 92.6% and a specificity of 100%. Median γ_{yx} increases with growing parameter A. (b) The reconstruction of the intrinsic RR time series is performed at a high level using both methods when respiration is paced. In the case of natural breathing the ARMAx filter outperforms the Gaussian notch filter. The ARMAx filter should be used in all scenarios.

An important observation is also the fact that intersubject variability, quantified as the IQR of the boxplots, does not present a clear dependency of breathing frequency but maximizes at 0.2 Hz. In addition, similar to the behavior observed for the median coupling value, the IQR is lowest for the breathing frequencies 0.1 and 0.6 Hz.

3.3.2. Fantasia database

In order to achieve a point of comparison between the PRS study and the Fantasia database, one segment of 3 min was chosen among the 120 min present in each recording of the Fantasia database. This is the same duration of signal in the PRS study. The segment was chosen to have ideal characteristics for the HRV analysis. For this purpose, Malik proposed three conditions that had to be fulfilled [38]:

- In the three minute interval no ectopic beats are present in the signal.
- No RR interval can differ in more than 20% from the previous or subsequent one.
- The RR time series must be stationary in the sense of Malik. In this definition, the first RR interval cannot differ in more than 20% from all other RR intervals in the segment.

In the case that more than one segment fulfilled the requirements, the Granger's causality γ_{yx} was calculated for all the valid segments and the one having median causality was chosen for further processing. Among the selected intervals used for coupling analysis, a median respiration rate of (0.3 ± 0.09) Hz was measured.

For the selected segment, the coupling measure γ_{yx} was calculated. This procedure was repeated for every subject in the database. The results obtained are depicted as a boxplot in Fig. 8. The threshold for significant coupling is also depicted in magenta. It can be observed that the median coupling among all subjects in the study is notoriously below the significant coupling threshold. However, a few of the subjects do present significant coupling. The intersubject variability is similar to the one observed in the PRS study for the breathing rate 0.3 Hz.

3.4. Analysis of heart rate variability

3.4.1. Paced respiration study

After significant coupling has been evaluated and proven, the separation of the respiration driven RR time series from the intrinsic RR time series was carried out. Afterwards, a comparison of the HRV parameters before and after the decoupling process was performed for all breathing rates. The results for two HRV parameters (SDNN and ApEn) are presented in Fig. 9 in the form of boxplots and all HRV parameters are summarized in Table 1. The statistical significance (p-value) of the comparison between parameter before and after decoupling was calculated using the paired Wilcoxon signed rank test. In general, we observed that the decoupling process generates an intrinsic RR time series that has less power than the one recorded from the ECG. We also saw that original HRV parameters have a strong dependency on the respiration rate. However, after decoupling, the median values decrease and tend to level (lower IQR) among all breathing frequencies. In addition, the intersubject variability is notoriously larger before decoupling than afterwards.

For the time domain parameters, we observed a significant reduction of SDNN and RMSSD values at lower breathing rates (0.1 and 0.2 Hz). Median remains almost constant at higher respiration frequencies (0.3–0.6 Hz). TINN has similar behavior as the one observed for SDNN. For the frequency domain parameters, we observe a strong decrease in LF power at a respiration rate of 0.1 Hz after decoupling. This is an interesting result that demonstrates that this method is potentially capable of separating sympathetic and parasympathetic activity in HRV even if they have

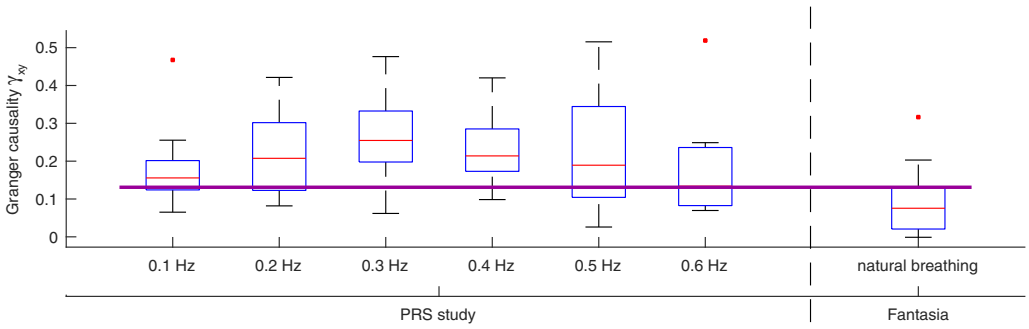

Fig. 8. Coupling measure based on Granger's cuasality γ_{yx} is displayed in dependency of the constant breathing frequency (PRS study) and natural breathing frequency (Fantasia database). Coupling proved to have a strong dependency on the respiration rate reaching its maximum at 0.3 Hz and its minimum (below threshold) for natural breathing.

Table 1
Summary of results obtained for the HRV parameters analyzed in this work. The table shows the parameter dependency of constant breathing frequency (PRS study) and natural breathing frequency (Fantasia database) before and after decoupling the respiration signal from the RR time series. The median value of each parameter together with its IQR can be seen in the table. A ratio between the values before and after the separation procedure can also be seen. The statistical significance (p-value) of the comparison between parameters before and after decoupling was obtained using the paired Wilcoxon signed rank test. In general, the process generates a decoupled RR time series that has less power than the one recorded originally from the ECG. In addition, HRV parameters proved to have a strong dependency on the respiration rate.

	0.1 Hz		0.2 Hz		0.3 Hz		0.4 Hz		0.5 Hz		0.6 Hz		Natural breathing	
	Median	IQR	Median	IQR	Median	IQR	Median	IQR	Median	IQR	Median	IQR	Median	IQR
SDNN [ms]	119.89	60.30	57.32	54.02	48.47	41.63	47.74	30.74	34.39	30.58	33.38	19.30	56.92	26.86
$SDNN_{dec}$ [ms]	61.63	32.75	44.53	27.33	40.75	31.85	43.39	26.27	32.41	31.97	30.46	16.66	52.90	35.37
ratio [no u.]	0.51	0.54	0.78	0.51	0.84	0.77	0.91	0.85	0.94	1.05	0.91	0.86	0.93	1.32
p-value	<**0.01**		<**0.01**		<**0.01**		<**0.01**		<**0.01**		<**0.01**		<**0.01**	
rMSSD [ms]	68.50	55.63	41.92	63.80	35.94	65.54	38.11	42.99	30.62	29.54	29.86	20.89	39.26	31.65
$rMSSD_{dec}$ [ms]	47.79	40.40	28.17	32.98	25.12	35.21	24.61	22.49	20.41	23.05	18.39	13.14	34.19	28.40
ratio [no u.]	0.70	0.73	0.67	0.52	0.70	0.54	0.65	0.52	0.67	0.78	0.62	0.63	0.87	0.90
p-value	<**0.01**		<**0.01**		<**0.01**		<**0.01**		<**0.01**		<**0.01**		<**0.01**	
LF [ms^2/Hz]	5791.03	3878.21	260.46	393.07	190.88	384.93	187.18	248.88	167.03	219.68	100.55	118.04	353.88	534.00
LF_{dec} [ms^2/Hz]	357.65	344.31	249.26	389.64	163.36	368.86	222.42	227.77	178.09	214.78	115.24	130.22	297.72	460.94
ratio [no u.]	0.06	0.09	0.96	0.99	0.86	0.96	1.19	0.92	1.07	0.98	1.15	1.10	0.84	0.86
p-value	<**0.01**		**0.04**		**0.01**		0.71		0.76		0.57		0.06	
HF [ms^2/Hz]	512.05	716.17	786.65	2042.61	325.30	757.02	66.53	117.57	34.87	44.58	18.43	16.98	158.74	267.40
HF_{dec} [ms^2/Hz]	438.64	602.99	97.36	198.31	58.74	166.43	49.24	61.47	35.32	47.47	22.91	26.03	111.58	167.30
ratio [no u.]	0.86	0.84	0.12	0.10	0.18	0.22	0.74	0.52	1.01	1.06	1.24	1.53	0.70	0.63
p-value	0.55		<**0.01**		<**0.01**		<**0.01**		0.30		0.42		0.06	
LF/HF [no u.]	9.89	9.16	0.27	0.28	0.86	1.39	2.72	1.33	5.02	3.16	5.63	3.80	1.87	3.76
LF/HF_{dec} [no u.]	0.58	0.92	2.50	2.63	3.32	2.55	4.67	2.44	4.68	2.54	5.42	4.18	2.30	3.97
ratio [no u.]	0.06	0.10	9.14	9.44	3.87	1.84	1.72	1.84	0.93	0.81	0.96	1.10	1.23	1.06
p-value	<**0.01**		<**0.01**		<**0.01**		<**0.01**		0.45		0.12		0.06	
TINN [ms]	396.69	240.55	278.48	193.93	228.63	178.01	232.32	148.07	179.82	128.32	164.36	82.11	253.05	102.71
$TINN_{dec}$ [ms]	291.95	146.65	221.37	111.26	194.18	146.23	199.10	101.96	160.02	141.81	144.10	67.36	225.23	120.83
ratio [no u.]	0.74	0.61	0.79	0.57	0.85	0.82	0.86	0.69	0.89	1.11	0.88	0.82	0.89	1.18
p-value	<**0.01**		<**0.01**		<**0.01**		<**0.01**		<**0.01**		**0.05**		0.12	
ApEn [no u.]	0.68	0.13	0.90	0.13	0.90	0.18	0.99	0.20	0.92	0.14	0.96	0.22	0.82	0.24
$ApEn_{dec}$ [no u.]	0.95	0.10	0.98	0.10	0.94	0.15	0.97	0.14	0.98	0.13	1.01	0.15	0.86	0.16
ratio [no u.]	1.40	0.76	1.09	0.73	1.04	0.82	0.98	0.68	1.06	0.87	1.05	0.70	1.05	0.68
p-value	<**0.01**		<**0.01**		0.55		0.14		**0.03**		**0.02**		**0.02**	

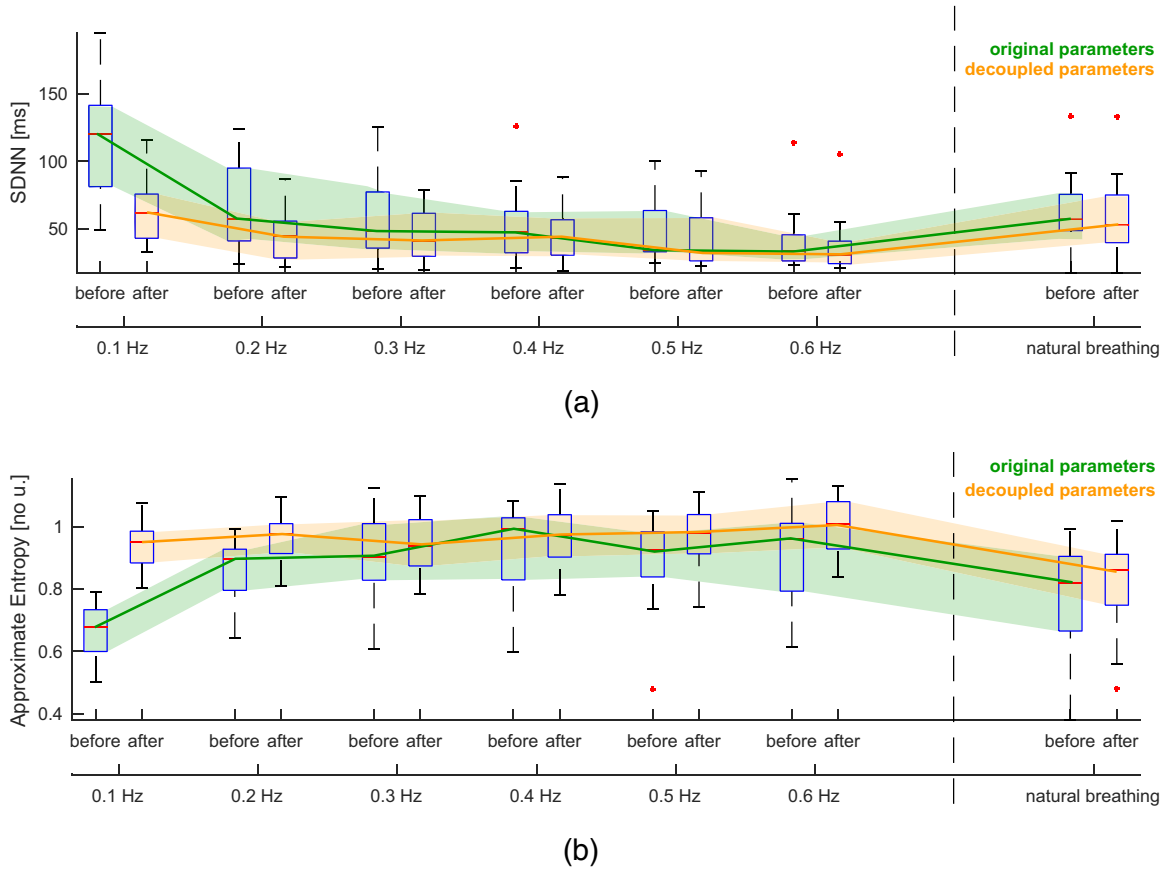

Fig. 9. (a) HRV parameter SDNN is displayed in dependency of the constant breathing frequency (PRS study) and for natural breathing (Fantasia database) before and after decoupling respiration. (b) HRV parameter SDNN is displayed in dependency of the constant breathing frequency (PRS study) and for natural breathing (Fantasia database) before and after decoupling respiration. A leveling of the boxplots can be observed after decoupling in both HRV parameters.

overlapping spectra. This result is also in accordance with the conclusions obtained from the simulation study.

Furthermore, the parameter HF is also notoriously diminished after decoupling in the rates 0.2 and 0.3 Hz. The nonlinear ApEn is the only parameter for which its median value increases after decoupling in every breathing rate. For this parameter, the largest changes are observed at lower breathing frequencies.

3.4.2. Fantasia database

The results obtained for the subjects in the Fantasia database can be seen in Fig. 9 and Table 1. Two of the HRV parameters (SDNN and ApEn) are presented in Fig. 9 in the form of boxplots and the results for the other HRV parameters are summarized in Table 1. The statistical significance (p-value) of the comparison between parameter before and after decoupling was calculated using the paired Wilcoxon signed rank test. In general, we also observed a slight decrease of the median HRV parameters and a reduction of IQR after decoupling. However, this reduction was not substantial, when compared to the initial values or the reduction observed in the PRS study.

4. Discussion

4.1. Validity of the model chosen to recreate coupling

The model chosen to recreate coupling has an open-loop structure and uses an FIR filter $G(k)$ to create a causal interaction between respiration (exogenous input) and the intrinsic RR time series to produce the measured heart period. This model is restrictive when compared to the capability of a full MDS model that allows more complex signal dependencies [26]. In particular, the exclusion of a closed-loop structure can be seen as a limitation because baroreflex and cardiopulmonary coupling are well known to be closed-loop interactions between heart rate, blood pressure and respiration [48]. In addition, methods based on closed-loop identification techniques, that asses also the quantification of direct and indirect coupling strength in all directions, has been proposed by Porta in the past [49]. Such models would deliver more information about the system structure and origin of cardiovascular oscillations but complicate the direct calculation of the Grangers causality in its original formulation as an improvement of predictability. Since our goal is to quantify exclusively the coupling strength from respiration to RR interval, our open loop model should be sufficient [49].

4.2. Evaluation of Granger's causality as a coupling measure

The Granger's causality based coupling measure $\gamma_{yx}^{5\%}$ proved to be, at least for the simulation study performed here, a reliable quantification of coupling. Among the 200 000 experiments performed in total, the parameter was able to correctly separate significant from non significant coupling in 96.3% of the cases. We also saw, that with increasing coupling strength (given by the parameter A), the median Granger's causality increased also and was above the significance threshold even for the lowest coupling strength $A = 0.6$. For larger parameter values of A the vast majority of cases were classified correctly which demonstrates the effectiveness of the theoretically derived threshold $\gamma_{yx}^{5\%}$. However, the method still struggled delivering many wrong classifications for the lowest coupling strength $A = 0.6$. This is probably due to fact that the energy of the respiration signal coupling into the RR time series is so low that

no significant improvement in the estimation process is observed, when respiration is considered. Nevertheless, this is a result that should not be problematic in practice. When coupling strength is low, the influence of respiration on the HRV parameter will also be low and decoupling will not modify the HRV parameters notoriously.

Furthermore, the model used to recreate the measured signals and its coupling is rather simple because of its linear nature. It is perfectly suited for a quantification technique also based on linear regression. Other types of models and signals are needed to deliver the ultimate validation of the method. Nevertheless, these results still convinced us of using $\gamma_{yx}^{5\%}$ to study coupling strength in the two databases presented in this work but keeping in mind that this value is a measure of linear coupling.

4.3. Evaluation of the separation algorithms

The results obtained from the theoretical evaluation of the separation algorithm demonstrated that, at least for the proposed simulation study, it is possible to reconstruct the intrinsic RR time series at a high level of accuracy. The MAx filter delivered better results in both scenarios, natural breathing and paced respiration. This is probably due to the fact that it is based on a coupling model that contains both, respiration and RR time series. The inclusion of both time series increases the available information and facilitates the estimation of the respiration derived RR time series, making it independent of the kind of respiration given. However, since the coupling interaction between signals is also modeled using linear combinations of past values, the decoupling algorithm might be overestimating the results.

The Gaussian notch filter is capable of reconstructing the intrinsic RR time series if respiration is paced. This is the kind of result that is expected for a band stop filter when the power spectrum of the breathing pattern is concentrated around a given frequency. However, in the more general case of spontaneous breathing, the Gaussian filter delivered notoriously worse results and larger variability. This is plausible because the filter was not developed for this kind of application. The larger the spread of the spectrum of the respiration signal is, the less capable the Gaussian filter is of reconstructing the intrinsic time series. Nevertheless, the Gaussian notch filter has the advantage of being applicable in the case that no respiration was recorded and the breathing rate can be considered to be constant. This filter is thus a low cost but acceptable solution in the case that a recording device for respiration is not available.

4.4. Coupling between RR time series and respiration

4.4.1. Paced respiration study

The results showed a clear dependency of median coupling strength from breathing rate. This is in accordance with other results reported in the literature [30]. However, the coupling strength can vary from very strong to not significant in the same group of subjects at a fixed respiration frequency. This lead us to believe, that the coupling strength could be a person specific characteristic that depends differently on the breathing frequency.

We also observed the strongest coupling at 0.3 Hz which is close to the natural breathing frequency of humans. These results reflect some sort of resonance for which coupling maximizes at the same frequency at which the subject would naturally breath. On the other hand, the lowest coupling strength at 0.1 Hz and 0.2 Hz could have different interpretations. First, a pure mathematical artifact can be theorized in which the AR part of the linear regression used to represent the RR time series is already very accurate. Thus, the introduction of the MAx part has low impact on the error variance leading to a smaller γ_{yx}. However, another more physiological explanation for this result can also be proposed. The baroreceptor reflex, together with other regulation mechanisms such as body temperature, systemic blood pressure, blood flow and perfusion are known to be localized below 0.2 Hz (typically around at 0.1 Hz) in the power spectrum of the RR time series [50,51]. These regulation mechanisms could somehow mask the influence coming from RSA on the time series and compromise its estimation.

We also saw that a decreasing coupling strength was present for respiration frequencies going from 0.4 to 0.6 Hz. This is also in accordance with the results presented in [15]. In that work was shown that RSA diminishes with increasing breathing rate.

4.4.2. Fantasia database

The results showed that the large majority (75%) of the subjects did not have significant coupling during spontaneous breathing. This is in part because of the older subjects who did not have a significant coupling at all, which is in accordance with the believe that RSA decreases with increasing age [16]. However, one half of the younger subjects had also no coupling. In addition, the median observed in the Fantasia database was lower than all other values observed in the PRS study. This result seems to demonstrates that physiological coupling appears to increase when paced respiration is present and diminishes during natural breathing. This is probably because paced respiration is not physiological but rather externally forced and very regular which could facilitate the synchronization of the breathing pattern and the heart rate. Furthermore, intersubject variability is in the same range as the one observed for 0.3 Hz in PRS study. This is an interesting result that could demonstrate that differences among subjects in their RSA are optimally estimated at their natural breathing frequency.

4.5. Analysis of heart rate variability

4.5.1. Paced respiration study

It was interesting to see how strong HRV parameters can depend on the paced breathing frequency. SDNN for example, which is a measure of total power in HRV, has a median value of 119.89 ms when breathing frequency is 0.1 Hz but it goes down below 40% of that original value at 0.4 Hz. In the hypothetical case that the SDNN value would be used for diagnostic purposes in a medical examination, the same patient could receive two completely different diagnosis depending on his breathing frequency and thus on the strength of coupling. Therefore, it was interesting to see how median values tend to level, when decoupling is applied. In addition, the intersubject variability was also smaller after decoupling. This result could help a physician to improve comparability among subjects because the data are more concentrated around its median.

Furthermore, the results show in general that after decoupling, a significant amount of HRV power was removed what demonstrates that RSA is responsible for a strong part of HRV when respiration is paced [52]. This reduction is an expected result because a significant part of the power was decoupled from the measured RR time series. However, depending on respiration rate, the HRV parameters are affected in different manners. For example, after decoupling SDNN at 0.1 Hz, it goes down to 50% of its original value, while at 0.4 Hz the decoupled parameter is above 90% of its previous measurement. However, this result is due to fact that SDNN tends to quantify the power located in the very low and low frequency bands. As respiration moves into the HF band, the impact on SDNN decreases.

Furthermore, the parameter LF is strongly diminished after decoupling when respiration rate is 0.1 Hz, while HF is notoriously affected when the breathing frequency is located in the interval from 0.2 to 0.4 Hz. This makes sense because these parameters are affected by localized spectral power in those same bands. Finally, the increase of ApEn at lower frequencies shows that the decoupled RR time series becomes more chaotic or less regular. This result is also plausible because the respiration driven RR time series is a very

repetitive signal. By removing it from the measured RR time series the decoupled one loses regularity.

4.5.2. Fantasia database

The results obtained from the Fantasia database demonstrated that the HRV parameters are notoriously less affected by RSA when breathing is natural. Small changes in HRV parameters are plausible because significant coupling was not present in a large portion of subjects. In addition, for the subjects that did present significant coupling, their coupling measure was also relatively small when compared to the results seen in the PRS study. Thus, we did not expect the separation algorithm to remove much power from the recorded RR time series and lead to significantly modified HRV parameters if the respiration driven variability had already low power. The small variations in IQR are also in accordance with the little power removed from HRV.

5. Limitations

From the methodological point of view, the algorithm presented here is based on linear regressions and least squares estimation that do not account for nonlinearities. Not only the breathing frequency, but also the breathing depth (amplitude) can have an influence on the coupling strength [15]. Neither the breathing amplitude nor other types of nonlinearities were included in the decoupling method presented here. In addition, the Granger's causality is a model based estimation of coupling and thus highly dependent on the model chosen. The order of the model is a relevant part of it that is estimated using the BIC. This is an optimization method that tends to favor lower orders. This can lead to an underestimation of the model that is not able to truly reproduce the behavior of the real system.

Even though an attempt was carried out to validate the methods at a theoretical level, the signal models used for the simulation study were rather simple. Signal coupling was modeled using linear combination of past values, which is specially convenient for a linear decoupling algorithm. In addition, RR time series was created using pink noise and respiration was given by a harmonic signal with varying frequency. Other more complex models that recreate the full behavior of the ANS can be found in literature [9]. However, for this particular application the signal models used and the results obtained were convincing and motivated the usage of the method on real data.

Even though the amount of subjects in the two studies presented in this paper is similar, 19 and 20 subjects respectively for the PRS study and Fantasia database, the group is heterogeneous and not particularly large. The PRS study is composed by rather young subjects, while the Fantasia database contains 10 young and 10 old subjects. In addition, in the PRS study participated significantly more men than women, while in the Fantasia database the same amount of subjects from each gender were present. For these reasons, the direct comparison between the results obtained from each study is not ideal. The results cannot be interpreted as golden truth but rather as hypothesis for future research. Ultimate validation can only be achieved in a larger prospective study.

Finally, it is worth mentioning that even though we tried to avoid aliasing related errors in our signal processing schemes, aliasing could still compromise the analysis up to some degree. Although the subjects that did not fulfill the sampling theorem with their mean heart rate were removed from the PRS study, the higher harmonics of the respiration signal are located outside the Nyquist band. However, according to the results observed in the simulation study where aliasing was not present, we expect these higher harmonics not to contain a significant amount of spectral power. Therefore, we believe the results obtained for the real measurements in this study are still accurate.

6. Future prospects

Primarily, the system theoretical description of the cardiorespiratory dynamics should be extended to include also blood pressure. Bidirectional interactions between RR time series, respiration and blood pressure should be achieved by building a closed feedback loop. Secondly, the coupling measure and separation algorithm presented here could be extended to account for nonlinear behavior (e.g. breathing depth) in the system. For this purpose, a new formulation of the problem together with a new algorithm is needed.

Furthermore, other relevant dependencies of the coupling strength and HRV parameters should be investigated. In this work we studied the influence of respiration rate and natural breathing, but the study could be extended to investigate other variables such as age, gender and fitness or health state of the subject. For such a research project more data are needed. Ideally, a new experiment should be designed from which the proposed variables can be investigated.

Additionally, it would be very interesting to study if the respiration free HRV parameters can be used to better quantify imbalances of the autonomic nervous system that are observed in many cardiac diseases such as diabetes mellitus, hypertension, myocardial infarction or chronic heart failure [53–56]. In those cases, a diminished HRV is a strong predictor for cardiac death. It could be of great medical use, if respiration free HRV parameter could predict mortality in a more accurate manner [19].

Finally, in order to deal with the possible aliasing problem that arises from the higher harmonics in the recorded RR time series but not in the respiration signal, we could postulate a new method in which the latter is resampled at the exact same points where the RR time series was sampled. By doing so, the aliasing effects would appear in both signals and affect them similarly. Thus, we could speculate that the coupling measure γ_{yx} and decoupling procedures could deliver even more accurate results.

7. Summary and conclusion

In this work, we developed a method to quantify coupling between RR time series and respiration. The method is based on Granger's causality and a value for the coupling strength and its statistical significance is computed. In the case of significant coupling, the separation of the respiration derived part of the RR time series is carried out using a MAx filter. For the particular case of paced respiration, we also implemented a Gaussian notch filter. These methods were validated at theoretical level using synthetic signals.

From the analysis of the PRS study, we observed that coupling varies depending on the respiration rate. The maximal coupling between respiration and RR time series was computed for a respiration rate of 0.3 Hz. For different respiration frequencies we also noted significantly different HRV parameters. From the analysis of HRV parameters after decoupling, we demonstrated that RSA is responsible for a strong part of HRV power when respiration is paced. We also observed that after decoupling, the HRV parameters tend to level among subjects. Thus, we concluded that one possible reason for intersubject variability in HRV could be due to different RSA strengths among subjects.

From the analysis of the Fantasia database, we learned that in the case of natural breathing, the coupling strength between respiration and RR time series is lower than for paced respiration and not significant in the majority of the subjects. This led us to believe that in the case of natural breathing the strength of RSA is lower

than for paced respiration. When the separation filter was applied for the subjects with significant coupling, we observed that the amount of power removed from the HRV is rather small and the HRV parameters remained almost constant. This led us to conclude, that the physiological mechanisms of cardiorespiratory coupling seem to potentiate during paced respiration and lower during natural breathing.

Finally, we propose that respiration free analysis of HRV during paced respiration might add new relevant insights to the interpretation of the HRV parameters, reduce intersubject variability and help better comprehension of the physiological or pathological processes that are related to them. However, more research is needed to definitely clarify the importance of a separated analysis of HRV with and without its respiration driven part.

References

[1] B.F. Robinson, S.E. Epstein, G.D. Beiser, E. Braunwald, Control of heart rate by the autonomic nervous system studies in man on the interrelation between baroreceptor mechanisms and exercise, Circ. Res. 19 (2) (1966) 400–411.
[2] P.K. Stein, M.S. Bosner, R.E. Kleiger, B.M. Conger, Heart rate variability: a measure of cardiac autonomic tone, Am. Heart J. 127 (5) (1994) 1376–1381.
[3] B. Friedman, J. Thayer, Autonomic balance revisited: panic anxiety and heart rate variability, J. Psychosom. Res. 44 (1) (1998) 133–151.
[4] M. Malik, T. Farrell, T. Cripps, A. Camm, Heart rate variability in relation to prognosis after myocardial infarction: selection of optimal processing techniques, Eur. Heart J. 10 (12) (1989) 1060–1074.
[5] W. Langewitz, H. Rüddel, H. Schächinger, Reduced parasympathetic cardiac control in patients with hypertension at rest and under mental stress, Am. Heart J. 127 (1) (1994) 122–128.
[6] N. Chattipakorn, T. Incharoen, N. Kanlop, S. Chattipakorn, Heart rate variability in myocardial infarction and heart failure, Int. J. Cardiol. 120 (3) (2007) 289–296.
[7] R. Bailón, P. Laguna, L. Mainardi, L. Sornmo, Analysis of heart rate variability using time-varying frequency bands based on respiratory frequency, in: EMBS 2007. 29th Annual International Conference of the IEEE Engineering in Medicine and Biology Society, 2007, IEEE, 2007, pp. 6674–6677.
[8] M. Garcí a-González, C. Vázquez-Seisdedos, R. Pallàs-Areny, Variations in breathing patterns increase low frequency contents in hrv spectra, Physiol. Measure. 21 (3) (2000) 417.
[9] M. Ursino, Interaction between carotid baroregulation and the pulsating heart: a mathematical model, Am. J. Physiol. – Heart Circulatory Physiol. 275 (5) (1998) H1733–H1747.
[10] R.S. Kronenberg, C.W. Drage, Attenuation of the ventilatory and heart rate responses to hypoxia and hypercapnia with aging in normal men, J. Clin. Investig. 52 (8) (1973) 1812.
[11] R.M. Berne, M.N. Levy, Cardiovascular Physiology, Mosby, 1967.
[12] B. Pomeranz, R.J. Macaulay, M.A. Caudill, I. Kutz, D. Adam, D. Gordon, K.M. Kilborn, A.C. Barger, D.C. Shannon, R.J. Cohen, H. Benson, Assessment of autonomic function in humans by heart rate spectral analysis, Am. J. Physiol. – Heart Circulatory Physiol. 248 (1) (1985) H151–H153.
[13] A. Ben-Tal, S. Shamailov, J. Paton, Evaluating the physiological significance of respiratory sinus arrhythmia: looking beyond ventilation-perfusion efficiency, J. Physiol. 590 (8) (2012) 1989–2008.
[14] F. Yasuma, J. Hayano, Respiratory sinus arrhythmia: why does the heartbeat synchronize with respiratory rhythm? Chest J. 125 (2) (2004) 683–690.
[15] J.A. Hirsch, B. Bishop, Respiratory sinus arrhythmia in humans: how breathing pattern modulates heart rate, Am. J. Physiol. – Heart Circulatory Physiol. 241 (4) (1981) H620–H629.
[16] J.B. Hellman, R.W. Stacy, Variation of respiratory sinus arrhythmia with age, J. Appl. Physiol. 41 (5) (1976) 734–738.
[17] W. Hrushesky, D. Fader, O. Schmitt, V. Gilbertsen, The respiratory sinus arrhythmia: a measure of cardiac age, Science 224 (4652) (1984) 1001–1004.
[18] A. Angelone, N.A. Coulter, Respiratory sinus arrhythmia: a frequency dependent phenomenon, J. Appl. Physiol. 19 (3) (1964) 479–482.
[19] M.T. La Rovere, G.D. Pinna, R. Maestri, A. Mortara, S. Capomolla, O. Febo, R. Ferrari, M. Franchini, M. Gnemmi, C. Opasich, et al., Short-term heart rate variability strongly predicts sudden cardiac death in chronic heart failure patients, circulation 107 (4) (2003) 565–570.
[20] I. Kawachi, D. Sparrow, P.S. Vokonas, S.T. Weiss, Decreased heart rate variability in men with phobic anxiety (data from the normative aging study), Am. J. Cardiol. 75 (14) (1995) 882–885.
[21] J. Choi, R. Gutierrez-Osuna, Removal of respiratory influences from heart rate variability in stress monitoring, Sensors J. IEEE 11 (11) (2011) 2649–2656.
[22] D. Widjaja, E. Vlemincx, S. Van Huffel, Stress classification by separation of respiratory modulations in heart rate variability using orthogonal subspace projection, in: Engineering in Medicine and Biology Society (EMBC) 2013. 35th Annual International Conference of the IEEE, IEEE, 2013, pp. 6123–6126.
[23] D. Widjaja, A. Caicedo, E. Vlemincx, I. Van Diest, S. Van Huffel, Separation of respiratory influences from the tachogram: a methodological evaluation, PLOS ONE 9 (7) (2014) e101713.
[24] A. Porta, P. Castiglioni, M. Di Rienzo, T. Bassani, V. Bari, L. Faes, G. Nollo, A. Cividjan, L. Quintin, Cardiovascular control and time domain granger causality: insights from selective autonomic blockade, Philos. Trans. R. Soc. London A: Math. Phys. Eng. Sci. 371 (1997) (2013) 20120161.
[25] E. Bowers, P. Langley, M. Drinnan, J. Allen, F. Smith, A. Murray, Simulation of cardiac RR interval time series, in: Computers in Cardiology, 2002, IEEE, 2002, pp. 233–236.
[26] G. Baselli, A. Porta, O. Rimoldi, M. Pagani, S. Cerutti, Spectral decomposition in multichannel recordings based on multivariate parametric identification, IEEE Trans. Biomed. Eng. 44 (11) (1997) 1092–1101.
[27] I.P. Castro, An Introduction to the Digital Analysis of Stationary Signals: A Computer Illustrated Text, CRC Press, 1989.
[28] K.C. Bilchick, R.D. Berger, Heart rate variability, J. Cardiovasc. Electrophysiol. 17 (6) (2006) 691–694.
[29] R.F. Schmidt, F. Lang, M. Heckmann, Physiologie des menschen: mit pathophysiologie, Springer-Verlag, 2007.
[30] M.V. Pitzalis, F. Mastropasqua, F. Massari, A. Passantino, R. Colombo, A. Mannarini, C. Forleo, P. Rizzon, Effect of respiratory rate on the relationships between rr interval and systolic blood pressure fluctuations: a frequency-dependent phenomenon, Cardiovasc. Res. 38 (2) (1998) 332–339.
[31] J. Lázaro, R. Bailón, P. Laguna, Y. Nam, K. Chon, E. Gil, Respiratory rate influence in the resulting magnitude of pulse photoplethysmogram derived respiration signals, in: Computing in Cardiology Conference (CinC), 2014, IEEE, 2014, pp. 289–292.
[32] P. PhysioBank, Physionet: components of a new research resource for complex physiologic signals [circulation electronic pages]/al goldberger, lan amaral, l. glass, jm hausdorff, Circulation 101 (23) (2000) e215–e220.
[33] N. Iyengar, C. Peng, R. Morin, A.L. Goldberger, L.A. Lipsitz, Age-related alterations in the fractal scaling of cardiac interbeat interval dynamics, Am. J. Physiol. – Regulat. Integr. Compa. Physiol. 271 (4) (1996) R1078–R1084.
[34] L. Sörnmo, P. Laguna, Bioelectrical Signal Processing in Cardiac and Neurological Applications, Academic Press, 2005.
[35] G.D. Clifford, F. Azuaje, P. McSharry, Advanced Methods and Tools for ECG Data Analysis, Artech House, Inc, 2006.
[36] G. Lenis, N. Pilia, T. Oesterlein, A. Luik, C. Schmitt, O. Dössel, P wave detection and delineation in the ECG based on the phase free stationary wavelet transform and using intracardiac atrial electrograms as reference, Biomed. Eng./Biomedizinische Technik 61 (1) (2016) 37–56.
[37] G. Lenis, T. Baas, O. Dössel, Ectopic beats and their influence on the morphology of subsequent waves in the electrocardiogram, Biomedizinische Technik/Biomed. Eng. 58 (2) (2013) 109–119.
[38] M. Malik, J. Bigger, A. Camm, R. Kleiger, A. Malliani, A. Moss, P. Schwartz, Heart rate variability standards of measurement, physiological interpretation, and clinical use, Eur. Heart J. 17 (3) (1996) 354–381.
[39] C.W. Granger, Investigating causal relations by econometric models and cross-spectral methods, Econometrica: J. Econom. Soc. (1969) 424–438.
[40] A. Porta, V. Bari, A. Marchi, B. De Maria, A.C. Takahashi, S. Guzzetti, R. Colombo, A.M. Catai, F. Raimondi, Effect of variations of the complexity of the target variable on the assessment of Wiener–Granger causality in cardiovascular control studies, Physiol. Meas. 37 (2) (2016) 276.
[41] J.K. Ghosh, M. Delampady, T. Samanta, An Introduction to Bayesian Analysis: Theory and Methods, Springer Science & Business Media, 2007.
[42] U. Richter, L. Faes, A. Cristoforetti, M. Masè, F. Ravelli, M. Stridh, L. Sörnmo, A novel approach to propagation pattern analysis in intracardiac atrial fibrillation signals, Ann. Biomed. Eng. 39 (1) (2011) 310–323.
[43] M. Kircher, G. Lenis, O. Dössel, Separating the effect of respiration from the heart rate variability for cases of constant harmonic breathing, Curr. Dir. Biomed. Eng. 1 (1) (2015) 46–49.
[44] P. Welch, The use of fast fourier transform for the estimation of power spectra: a method based on time averaging over short, modified periodograms, IEEE Trans. Audio Electroacoust. (1967) 70–73.
[45] D. Nunan, G.R. Sandercock, D.A. Brodie, A quantitative systematic review of normal values for short-term heart rate variability in healthy adults, Pacing Clin. Electrophysiol. 33 (11) (2010) 1407–1417.
[46] F.N. Fritsch, R.E. Carlson, Monotone piecewise cubic interpolation, SIAM J. Numer. Anal. 17 (2) (1980) 238–246.
[47] U.R. Acharya, K.P. Joseph, N. Kannathal, C.M. Lim, J.S. Suri, Heart rate variability: a review, Med. Biol. Eng. Comput. 44 (12) (2006) 1031–1051.
[48] A. Porta, F. Aletti, F. Vallais, G. Baselli, Multimodal signal processing for the analysis of cardiovascular variability, Philos. Trans. R. Soc. London A: Math. Phys. Eng. Sci. 367 (1887) (2009) 391–409.
[49] A. Porta, T. Bassani, V. Bari, E. Tobaldini, A.C. Takahashi, A.M. Catai, N. Montano, Model-based assessment of baroreflex and cardiopulmonary couplings during graded head-up tilt, Comput. Biol. Med. 42 (3) (2012) 298–305.
[50] H.D. Kvernmo, A. Stefanovska, M. Bracic, K.A. Kirkebøen, K. Kvernebo, Spectral analysis of the laser doppler perfusion signal in human skin before and after exercise, Microvasc. Res. 56 (3) (1998) 173–182.
[51] P. Stein PhD, R. Kleiger MD, Insights from the study of heart rate variability, Annu. Rev. Med. 50 (1) (1999) 249–261.
[52] H.-S. Song, P.M. Lehrer, The effects of specific respiratory rates on heart rate and heart rate variability, Appl.Psychophysiol. Biofeedback 28 (1) (2003) 13–23.

[53] E.B. Schroeder, L.E. Chambless, D. Liao, R.J. Prineas, G.W. Evans, W.D. Rosamond, G. Heiss, Diabetes, glucose, insulin, and heart rate variability the atherosclerosis risk in communities (aric) study, Diabetes Care 28 (3) (2005) 668–674.
[54] P.G. Guyenet, The sympathetic control of blood pressure, Nat. Rev. Neurosci. 7 (5) (2006) 335–346.
[55] S. Webb, A. Adgey, J. Pantridge, Autonomic disturbance at onset of acute myocardial infarction, BMJ 3 (5818) (1972) 89–92.
[56] G. Grassi, G. Seravalle, B.M. Cattaneo, A. Lanfranchi, S. Vailati, C. Giannattasio, A. Del Bo, C. Sala, G.B. Bolla, M. Pozzi, et al., Sympathetic activation and loss of reflex sympathetic control in mild congestive heart failure, Circulation 92 (11) (1995) 3206–3211.